**Supporting Information**

# Iron incorporation-induced nickel hydroxide multiphase with 2D/3D hierarchical sheet-on-sheet structure for electrocatalytic water oxidation

Pin Hao,‡[a]* Wenqian Zhu,‡[a] Liyi Li,[b] Ying Xin,[a] Junfeng Xie,[a] Fengcai Lei,[a] Jian Tian,[c] and Bo Tang[a]*

[a] College of Chemistry, Chemical Engineering and Materials Science, Collaborative Innovation Center of Functionalized Probes for Chemical Imaging in Universities of Shandong, Key Laboratory of Molecular and Nano Probes, Ministry of Education, Shandong Provincial Key Laboratory of Clean Production of Fine Chemicals, Shandong Normal University, Jinan 250014, P. R. China. E-mail: tangb@sdnu.edu.cn, haopin@sdnu.edu.cn

[b] Intel Corporation, Hillsboro, OR 97124, United State.

[c] School of Materials Science and Engineering, Shandong University of Science and Technology, Qingdao 266590, P. R. China.

‡ These authors contributed equally to this work

## Experimental

### Modification of the pristine carbon cloth

For obtaining the porous surface, the pristine carbon cloths (1 ×4 $cm^2$) were immersed in the concentrated $HNO_3$ for 30 min firstly and ultrasonically rinsed with deionized (DI) water to get rid of the surface oxides. Then, the above carbon cloths were put into a 50 ml Teflon-lined stainless-steel autoclave with 40 mL $Ni(NO_3)_2$ $6H_2O$ (0.25 M) and hexamine (0.5 M) aqueous solution, and heated in an oven at 120 $^oC$ for 10 h. Then, the carbon cloths were stayed after cooling and cleaned residue reagent with ethanol. Followed drying, the samples were calcined at 900 ℃ for 90 min under the protection of $N_2$ in a tube furnace at the heating rate of 10 °C$min^{-1}$. Finally, the above carbon cloths were soaked in the concentrated HCl for 12 h and then washed by DI water and ethanol for several times to obtain the etched porous carbon cloths (described as CC).

### Synthesis of Fe incorporated $Ni(OH)_2$ multiphase on CC (Fe:$Ni(OH)_2$ MP/CC)

The Fe:$Ni(OH)_2$ MP/CC catalysts with variable molar ratios of Fe and Ni were fabricated via an electrochemical deposition method in the salt solution of Ni/Fe and followed by a hydrothermal process. Firstly, the Fe-Ni precursor was obtained by electrochemical deposition process in a 100 ml aqueous solution containing 2 mM $Fe(NO_3)_3$ $9H_2O$ and 6 mM $Ni(NO_3)_2$ $6H_2O$ as the electrolyte, which was performed at -1.0 V (vs SCE) for 10 minutes in a three-electrode system. CC and platinum plate are used as working electrode and counter electrode, respectively. Followed by the deposition, Fe-Ni precursors were washed by DI water and dried in an oven for 10 h (named as Fe-Ni/CC). Subsequently, 6 mmol dicyandiamide was dissolved and stirred for 30 min in 40 ml DI water to form the transparent aqueous solution, and then poured into a 50 ml Teflon-lined stainless-steel autoclave. One piece of Fe-Ni/CC precursor was placed into the above autoclave, and then sealed to maintain at 120 $^oC$ for 8 h. After washing with DI water and drying in vacuum, iron incorporated $Ni(OH)_2$ multiphase with 2D/3D hierarchical sheet-on-sheet nanostructure on CC was obtained (represented as Fe:$Ni(OH)_2$ MP/CC 1:3). Different concentrations of iron in $Ni(OH)_2$ multiphase were realized by controlling the molar ratio of Fe and Ni in the electrolyte (0 mM $Fe(NO_3)_3$ $9H_2O$ and 6 mM $Ni(NO_3)_2$ $6H_2O$, 2 mM $Fe(NO_3)_3$ $9H_2O$ and 4 mM $Ni(NO_3)_2$ $6H_2O$, 2 mM $Fe(NO_3)_3$ $9H_2O$ and 8 mM $Ni(NO_3)_2$ $6H_2O$), denoted as β-$Ni(OH)_2$/CC, Fe:$Ni(OH)_2$ MP/CC 1:2 and Fe:$Ni(OH)_2$ MP/CC 1:4, respectively.

### Synthesis of α-$Ni(OH)_2$/β-$Ni(OH)_2$ nanosheets on CC

The α-$Ni(OH)_2$/β-$Ni(OH)_2$ nanosheets grown on CC were prepared through the chemical bath deposition method.[1] Typically, the substrate of CC was placed into a 45 mL aqueous solution containing 5.26 g $NiSO_4$ $6H_2O$ and 1 g $K_2S_2O_8$. Then, the solution was stirred for several minutes with the addition of 5 mL $NH_3H_2O$ (30-33 wt%) drop by drop. After standing the above mixture at room temperature for 2 h, the coated CC was taken out and rinsed with DI water, and then dried in air (denoted as α/β $Ni(OH)_2$/CC).

**Synthesis of α-$Ni(OH)_2$ nanosheets on CC**

α-$Ni(OH)_2$ nanosheets were prepared according to our previous report.[2] In a typical synthesis, one piece of CC was placed into a 100 ml Teflon-lined stainless-steel autoclave containing 0.6 mmol $Ni(NO_3)_2$ $6H_2O$ in 90 ml DI water. Then, the autoclave was sealed and heated at 120 $^oC$ for 12h. After washing with DI water and drying in vacuum, α-$Ni(OH)_2$ nanosheets on CC were obtained (represented as α-$Ni(OH)_2$/CC).

**Structural Characterization**

The field-emission scanning electron microscope (FE-SEM, Hitachi SU8010A) was employed to characterize the morphology of catalyst. Detailed microstructure was recorded using the high-resolution transmission electron microscopy (HRTEM, JEOL JEM2100F). The phase of samples was studied through the X-ray powder diffraction (XRD) using a Philips X'Pert Pro Super diffractometer with Cu Kα radiation (λ = 1.54178 Å). The diffraction peaks intensity of carbon is so strong that the characteristic peaks of $Ni(OH)_2$ can't be observed. So in order to eliminate the interference of carbon, the sample was put in the DI water with ultrasonic treatment for 10 min, and then dropped the ultrasonic water on a glass slide and dried in an oven. Then we repeated the drop operation on the slide for five times and used the obtained slide to investigate the phase of catalysts using XRD measurement. The X-ray photoelectron spectroscopy (XPS) measurement was carried on a X-ray photoelectron spectrometer system (Thermo Scientific ESCLAB250Xi). The energy dispersive spectrometer (EDS) and the X-ray electron probe microanalyzer (EPMA-1720H, Shimadzu) were performed to investigate the distribution of elements. The inductively coupled plasma optical emission spectroscope (ICP-OES, Perkin Elmer Optima 7300DV) was carried out to identify the molar ratios of Fe and Ni in the catalysts. The thickness of nanosheets was measured using the atomic force microscopy (AFM) on a Cypher VRS AFM equipment (Oxford Instruments).

**Electrocatalytic measurements**

The OER catalytic behaviour of catalysts was measured in the three-electrode set-up and the measured potentials were converted to a reversible hydrogen electrode (RHE) based on the equation of $E_{vs\ RHE} = E_{vs\ Hg/HgO} + E^{o}_{Hg/HgO} + 0.059pH$. All potentials involved in this study are referred to RHE except where noted, and all the data are revealed without IR correction. The obtained catalysts were applied as the working electrode directly without binder. The reference electrode and the counter electrode are the Hg/HgO electrode and the platinum gauze (2 × 2 $cm^2$, 60 mesh), respectively. The cyclic voltammetry (CV) and the linear sweep voltammetry (LSV) curves were recorded on the electrochemical workstation (CHI660E) with the scan rate of 2 mV $s^{-1}$ in the 1 M KOH electrolyte. The electrochemical impedance spectroscopy (EIS) test was conducted at 1.5 V under the frequencies from 0.01 Hz to 100 kHz. The stability was detected via the chronoamperometry measurement and the long-term cyclic voltammetry test.

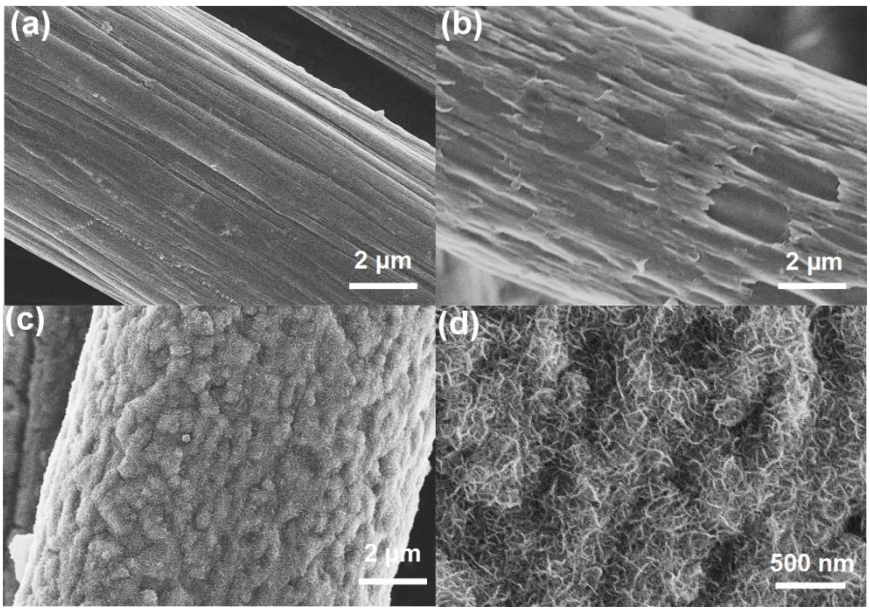


Fig.S1 SEM images of (a) pristine carbon cloths, (b) etched carbon cloths (CC), (c, d) Fe-Ni precursors on etched carbon cloths.

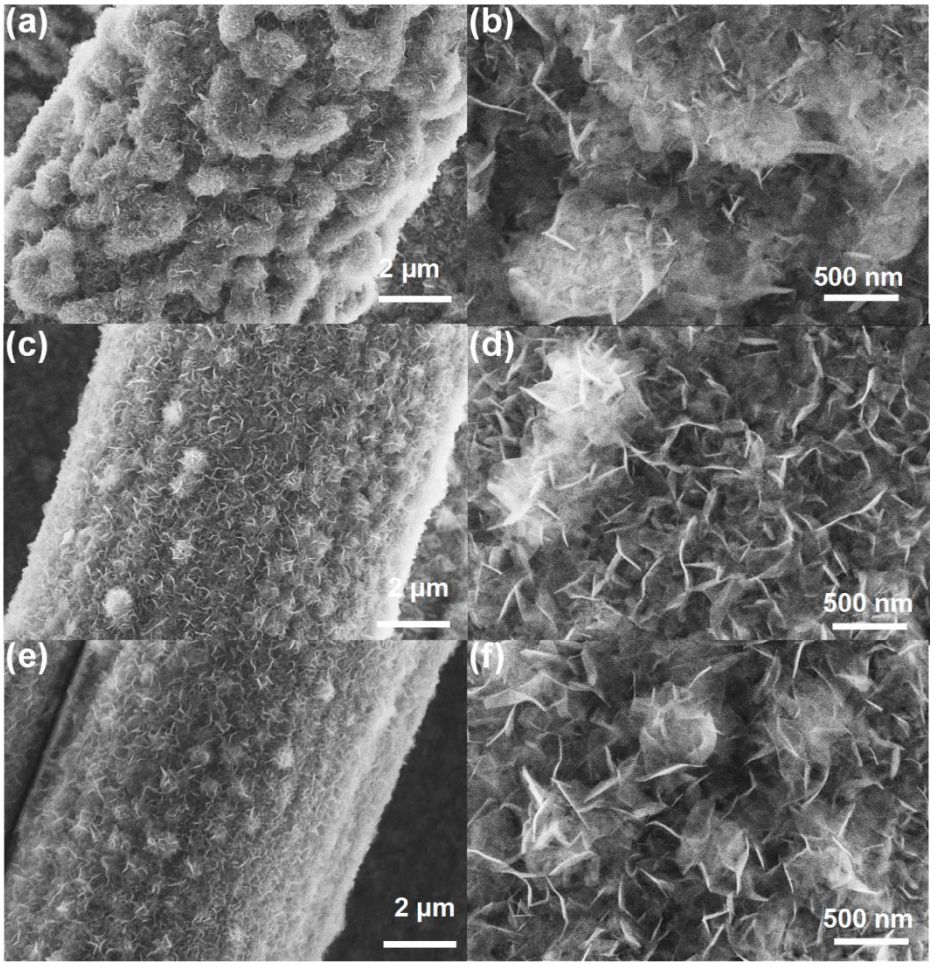


Fig.S2 SEM images of (a, b) β-$Ni(OH)_2$/CC, (c, d) Fe:$Ni(OH)_2$ MP/CC 1:2, and (e, f) Fe:$Ni(OH)_2$ MP/CC 1:4.

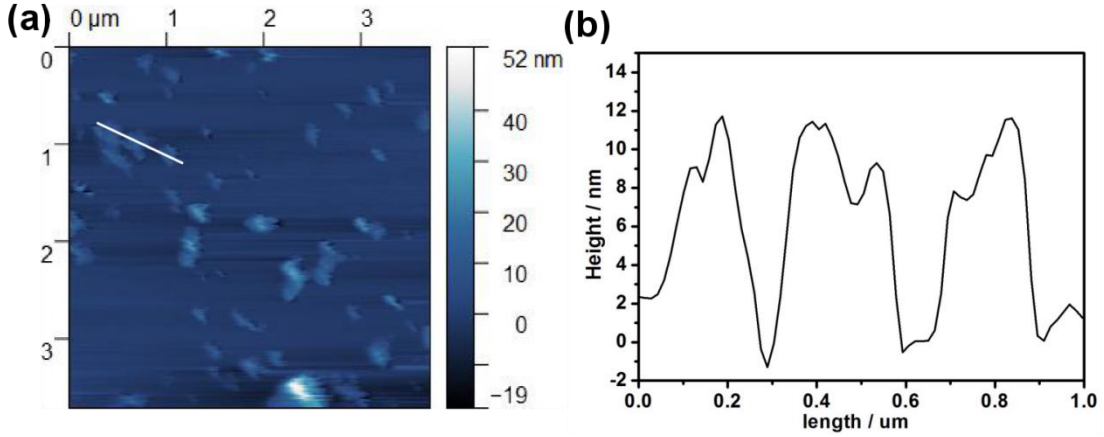


Fig.S3 (a) AFM image and (b) the height profile of Fe:$Ni(OH)_2$ MP/CC 1:3.

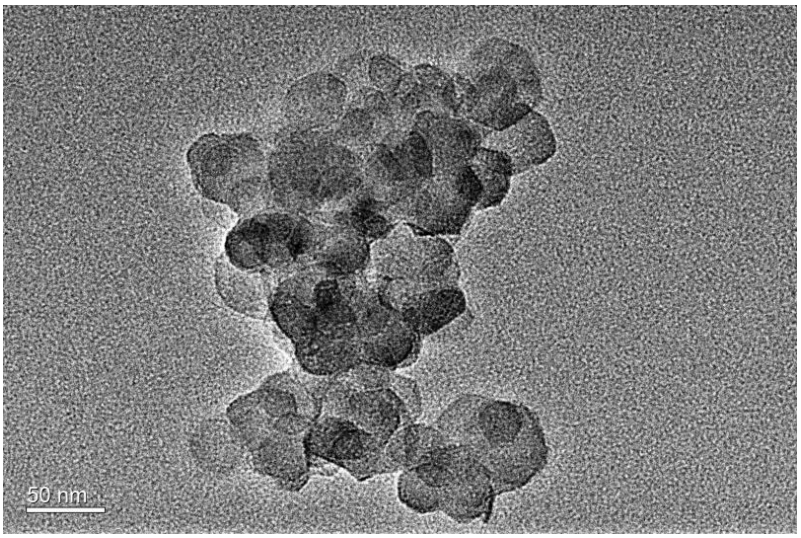


Fig.S4 TEM image of Fe:$Ni(OH)_2$ MP/CC 1:3 without vertically aligned nanosheets.

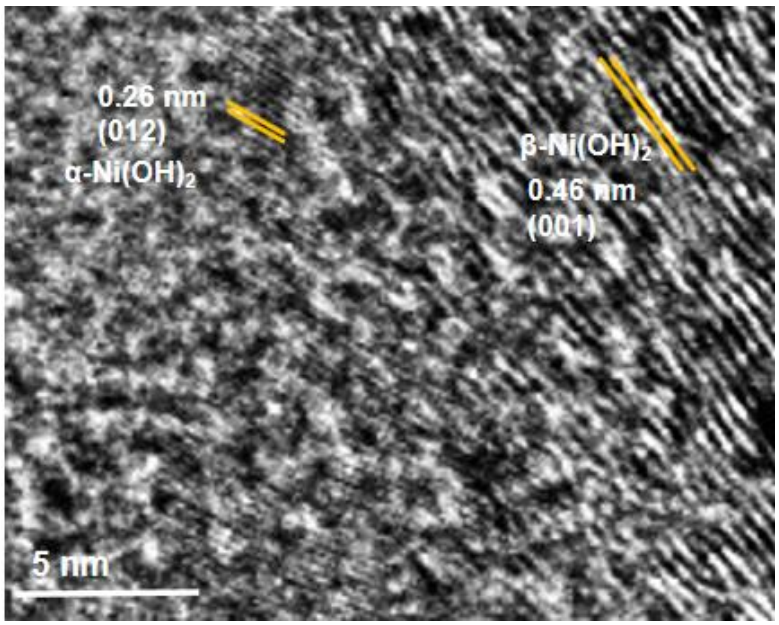


Fig.S5 The partial enlarged TEM image of the Fe:$Ni(OH)_2$ MP/CC 1:3 sample.

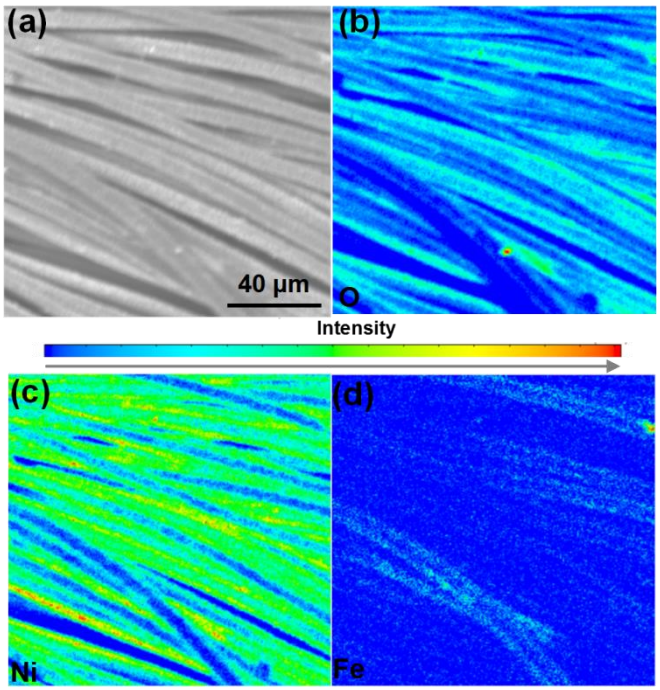


Fig.S6 EPMA images of the sample (Fe:$Ni(OH)_2$ MP/CC 1:3), (a) the morphological image, (b) element mapping of O, (c) Ni, (d) Fe.

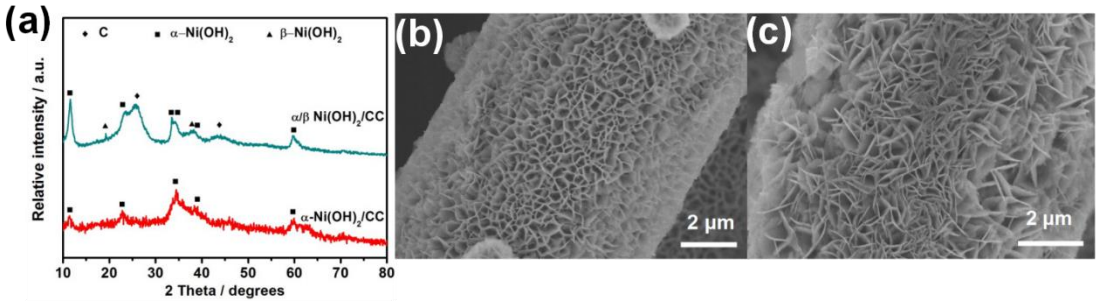


Fig.S7 Phase and morphological characterization of α/β $Ni(OH)_2$/CC and α-$Ni(OH)_2$/CC: (a) XRD patterns, SEM images of (b) α/β $Ni(OH)_2$/CC, (c) α-$Ni(OH)_2$/CC.

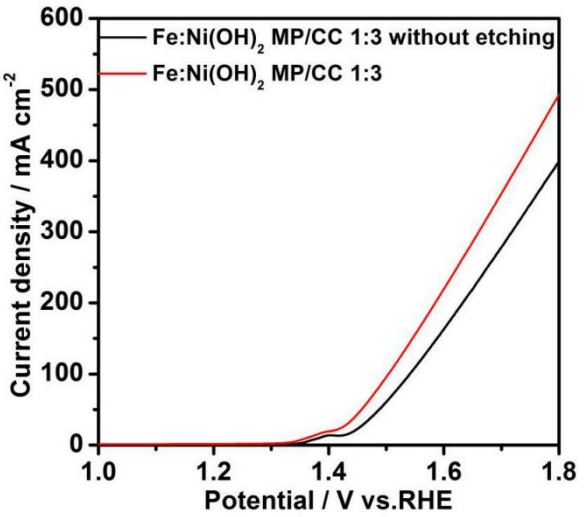


Fig.S8 LSV curves of the Fe:Ni(OH)$_2$ MP 1:3 catalyst grown on the carbon cloths with and without etching.

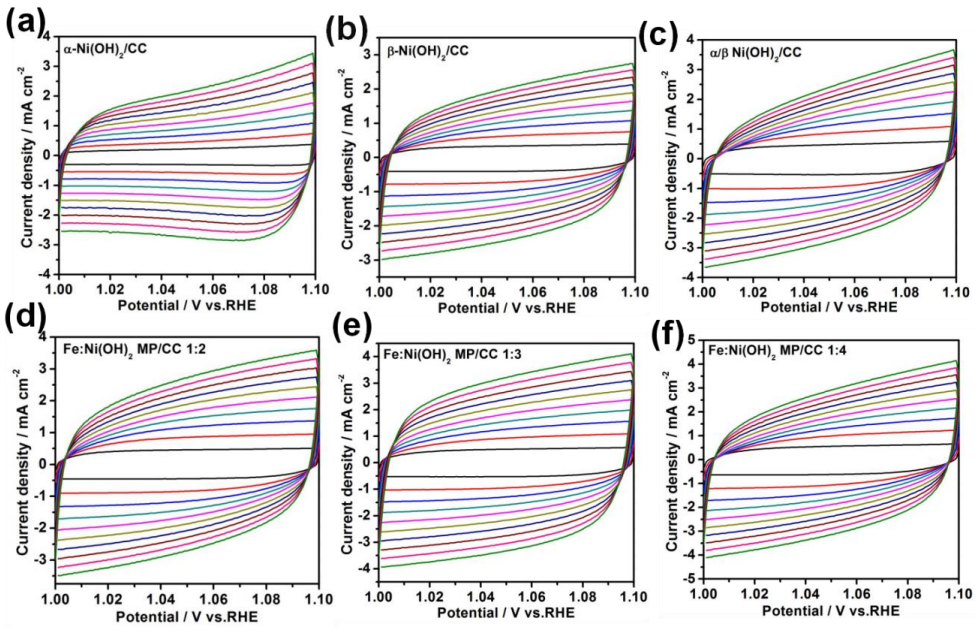


Fig.S9 CV curves of the samples at various scan rates from 10-100 mV $s^{-1}$ in non-redox region.

The investigation of the electrochemical surface area (ECSA) of the catalysts was accomplished according to the reported paper.[3] Since electrochemical double-layer capacitance ($C_{dl}$) is proportional to ECSA, $C_{dl}$ values were measured by cyclic voltammetry (CV) curves vs. various scan rates from 10 to 100 mV $s^{-1}$ at non-redox region (1.0-1.1 V vs. RHE) , which could be considered as the double-layer capacitive behaviour (Fig.S9). The $C_{dl}$ value is estimated by plotting the $\Delta J$ ($J_a$-$J_c$) at 1.05 V vs. RHE against scan rates, where the value of slope is twice $C_{dl}$.

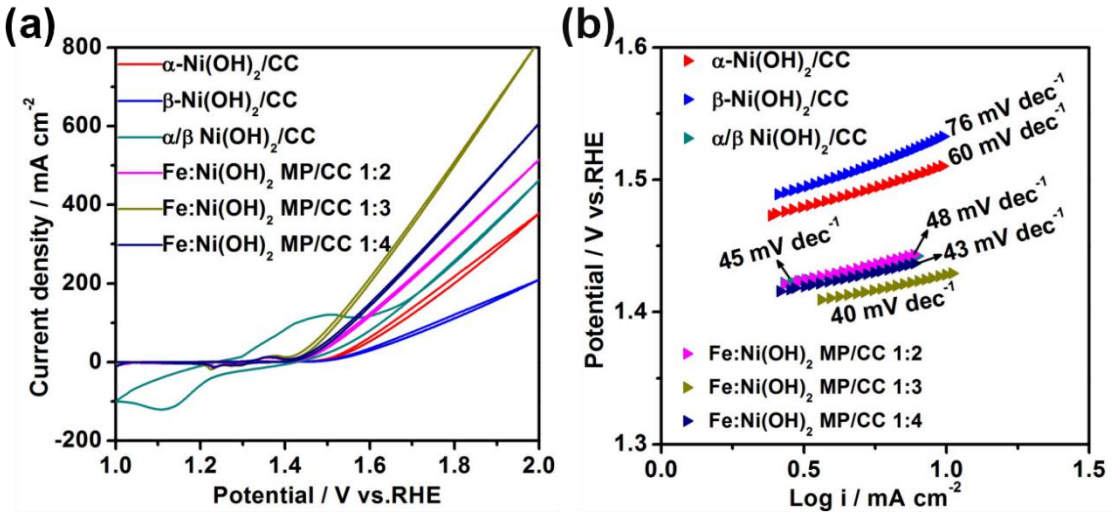


Fig.S10 (a) CV curves of the samples at the scan rate of 2 mV $s^{-1}$, (b) Tafel plots derived from the cathodic sweep of CV curves.

**Table S1.** The content of Ni in the etched carbon cloth derived from the ICP analysis.

| Sample | Atomic% of Ni |
|---|---|
| CC | 0 |

**Table S2.** Molar ratios of Ni and Fe in the samples derived from the ICP analysis.

| Sample | Molar ratio of Fe and Ni | Concentration of Fe (Fe/(Fe+Ni) wt%) |
|---|---|---|
| β-$Ni(OH)_2$/CC (without doping) | 0 | 0 |
| Fe:$Ni(OH)_2$ MP/CC 1:2 | 1:28.36 | 3.41 |
| Fe:$Ni(OH)_2$ MP/CC 1:3 | 1:40.28 | 2.42 |
| Fe:$Ni(OH)_2$ MP/CC 1:4 | 1:53.54 | 1.83 |

**Table S3**. Comparison of catalytic activity for OER on different catalysts.

| Catalyst | Current density at 1.8 V (mA $cm^{-2}$) | Overpotential at 100 mA $cm^{-2}$ (mV) | Reference |
|---|---|---|---|
| pa-NiFe LDH NS/NIF | ~350 | 326 | 4 |
| a-$NiFeO_x$/NIF | ~325 | 366 | 4 |
| $NiFe_2O_4$ NP/NIF 0.1% | ~165 | 453 | 4 |
| Fe:a-$Ni(OH)_2$/NF F:a-$Ni(OH)_2$ | ~200 | >400 | 5 |
| Ni-N-O | NA | >470 | 6 |
| F:$Ni(OH)_2$ / $Ni_3S_2$ | NA | >370 | 7 |
| $NiCo_2S_4$ NW/NF | 340 | 360 | 8 |
| Hollow nanoprisms based on NiFe LDH | NA | ~320 | 9 |
| $Ni_2P$ hollow microspheres | NA | ~320 | 10 |
| α-$Ni(OH)_2$/CC | ~100 | ~570 | 11 |
| β-$Ni(OH)_2$/CC | 199.36 | 430 | This work |
| α/β $Ni(OH)_2$/CC | 113.29 | 530 | This work |
| Fe:$Ni(OH)_2$ MP/CC 1:2 | 258.05 | 390 | This work |
| Fe:$Ni(OH)_2$ MP/CC 1:3 | 303.86 | 340 | This work |
| Fe:$Ni(OH)_2$ MP/CC 1:4 | 492.89 | 270 | This work |
| | 366.65 | 320 | This work |

Note: "~" stands for the estimated value from the LSV curves.

**Table S4.** The fitted values of $R_s$ and $R_{ct}$ derived from the EIS test.

| Sample | $R_s$ | $R_{ct}$ |
|---|---|---|
| β-$Ni(OH)_2$/CC | 4.17 | 12.89 |
| Fe:$Ni(OH)_2$ MP/CC 1:2 | 4.21 | 4.40 |
| Fe:$Ni(OH)_2$ MP/CC 1:3 | 2.64 | 1.52 |
| Fe:$Ni(OH)_2$ MP/CC 1:4 | 3.87 | 4.11 |
| α/β $Ni(OH)_2$/CC | 4.26 | 5.49 |
| α-$Ni(OH)_2$/CC | 4.21 | 6.42 |

## Reference


1. N. A. Alhebshi, R. B. Rakhi and H. N. Alshareef, *Journal of Materials Chemistry A*, 2013, **1**, 14897-14903.
2. J. Xie, W. Liu, F. Lei, X. Zhang, H. Qu, L. Gao, P. Hao, B. Tang and Y. Xie, *Chemistry – A European Journal*, 2018, **24**, 18408-18412.
3. J. Xie, J. Zhang, S. Li, F. Grote, X. Zhang, H. Zhang, R.Wang, Y. Lei, B. Pan and Y. Xie, *Journal of the American Chemical Society*, 2013, **135**, 17881-17888.
4. J. Xie, H. Qu, F. Lei, X. Peng, W. Liu, L. Gao, P. Hao, G. Cui and B. Tang, *Journal of Materials Chemistry A*, 2018, **6**, 16121-16129.
5. J. Xie, W. Liu, F. Lei, X. Zhang, H. Qu, L. Gao, P. Hao, B. Tang and Y. Xie, *Chemistry – A European Journal*, 2018, **24**, 18408-18412.
6. N. Hussain, W. Yang, J. Dou, Y. Chen, Y. Qian and L. Xu, *Journal of materials chemistry A*, 2019, **7**, 9656-9664.
7. J. Huang, Y. Sun, X. Du, Y. Zhang, C. Wu, C. Yan, Y. Yan, G. Zou, W. Wu and R. Lu, *Advanced materials*, 2018, **30**, 1803367.
8. P. Hao, W. Zhu, F. Lei, X. Ma, J. Xie, H. Tan, L. Li, H. Liu and B. Tang, *Nanoscale*, 2018, **10**, 20384-20392.
9. A. Sivanantham , P. Ganesan and S. Shanmugam, *Advanced Functional Materials*, 2016, **26**, 4661-4672.
10. L. Yu, J. Yang, B. Guan, Y. Lu and X. W. Lou, *Angewandte Chemie International Edition*, 2018, **57**, 172-176.
11. H. Lei, M. Chen, Z. Liang, C. Liu, W. Zhang and R. Cao, *Catalysis Science & Technology*, 2018, **8**, 2289-2293.